Discrimination and Interpretation of Spectral Phenomena by Room-Temperature Single-Molecule Spectroscopy

Christian Blum,[†] Frank Stracke,[†] Stefan Becker,[‡] Klaus Müllen,[‡] and Alfred J. Meixner*[,‡]

Physikalische Chemie, Universität Siegen, 57068 Siegen, Germany, and Max Planck Institut für Polymerforschung, Ackermannweg 10, 55128 Mainz, Germany

Received: August 29, 2000; In Final Form: February 7, 2001

The single-molecule fluorescence properties of the two perylenediimide dyes, 9-amino-*N*-(2,6-diisopropylphenyl)perylene-3,4-dicarboximide (API), and the derivative *N*,*N*-di(*tert*-butoxycarbonyl)-API (DAPI), are investigated in the amorphous host polystyrene at room temperature. For API, three spectroscopically different types of spectra can be distinguished, two of them can be assigned to the off-resonance and the in-resonance conformer of the amino group and the chromophore's π-electron system, repectively. The bathochromic third spectrum is suggested to originate also from an off-resonance conformer. In accordance with the sterically demanding substituents only off-resonance spectra are found for DAPI. Not being limited by the inhomogeneous spectral distribution, many molecules show clearly resolved vibronic structure and can be characterized by their spectral means, the vibronic maxima positions, and the vibronic band gaps. Sequences of consecutive spectra reveal different forms of dynamic behavior such as diffusion and abrupt jumps, both in the spectral domain and in the intensity trajectories. These can be summarized in a rough classification of the observed dynamic phenomena.

Introduction

Much interest has recently been in spectral fluctuations observed in single-molecule spectroscopy. Since the optical properties of a dye molecule depend very sensitively on the interaction with the surrounding host molecules, the analysis of the dynamic behavior of the fluorescence spectrum or emission rate has the potential to reveal dynamic molecular processes else obscured in a bulk measurement due to ensemble averaging. (For reviews on single molecule spectroscopy consult, for example the references 1−5). This offers the possibility to use single molecules as local sensors to probe, for example, the local pH,[6] the kinetics of enzymatic reactions,[7−9] or the conformational dynamics of biomolecules by fluorescence resonance energy transfer.[8,9] The fluorescence dynamics of single molecules was investigated to study energy transfer in multichromophoric dendrimeres[10] and to explore the photophysics of fluorescent proteins.[11]

Single-molecule fluorescence dynamics has mostly been analyzed by means of fluorescence correlation spectroscopy and histograms on dark state durations, yielding correlation times and rate constants of underlying photophysical processes from seconds to nanoseconds,[12−15] and fluorescence polarization spectroscopy for probing the rotational diffusion[16,] and structural deformations of multichromophoric systems.[17] Many interesting molecular processes, such as chemical reactions or conformational changes, lead to spectral changes large enough to be observed at room temperature. Still the analysis of fluctuations in the spectral domain is less common, probably due to the rather long integration time needed for acquiring spectra with a decent signal-to-noise ratio. Yet a time resolution of 1 s can reveal a multitude of spectral dynamics. Thus, analyzing sequences of consecutive spectra of one molecule makes it possible to study interesting spectral phenomena like spectral and intensity variations as well as changes in the intensity ratio between vibronic bands. Furthermore, single-molecule spectroscopy can reveal spectroscopically different forms of one dye which are present in the same sample and hence are difficult to distinguish in a bulk measurement such as the contact ion-pair of rhodamine dyes[18] or different conformers of the same dye.[19]

Here we investigate in depth the fluorescence properties of the two perylenediimide dyes, 9-amino-*N*-(2,6-diisopropylphenyl)perylene-3,4-dicarboximide (API) and its derivative *N*,*N*-di(*tert*-butoxycarbonyl)-API, by means of single-molecule spectroscopy in polystyrene at room temperature. Not being limited by the inhomogeneous spectral distribution the fluorescence spectra of many molecules show clearly resolved vibronic structure. Hence these spectra can easily be characterized by various parameters. These parameters are statistically analyzed to yield specific conclusions like vibronic energy band gaps or vibronic maxima positions, for the investigated dye−host system. The analysis of sequences of spectra with high vibronic resolution allows a basic classification of the observed dynamic phenomena.

Experimental Section

All studies were performed with a confocal fluorescence microscopy setup, based on a Zeiss Axiovert 135 TV. For focusing the excitation light and for collecting the fluorescence light the same microscope objective (Plan-Neofluar, 100*x*/1.30 oil, Zeiss) was used. Raster scanning and positioning with nanometer precision of the sample was done by a feedback-controlled sample stage (PI, P-517.K008). A single line argon-ion-laser (American Laser Corporation 60X-200, at 514.5 nm)

* Corresponding author. Universität Siegen, Physikalische Chemie, Adolf Reichwein Strasse 2, 57068 Siegen, Germany. Fax: +49-271-7402805. E-mail: meixner@mail.pc.chemie.uni-siegen.de.

[†] Physikalische Chemie.

[‡] Max Planck Institut für Polymerforschung.

10.1021/jp0031092 CCC: $20.00
Published on Web 07/03/2001

served as excitation light source. An acoustooptic modulator (Brimrose TEM-85-10) was used to couple the excitation light into the microscope during data acquisition. To cut off background luminescence from the laser tube, a narrow band interference filter (L. O. T.-Oriel GmbH, $\lambda_{max} = 515$ nm, fwhm $= 3.3$ nm) was applied. The collected fluorescence light was separated from scattered excitation light by a dichroic mirror (Zeiss FT510) and a holographic notch filter (Kaiser Optical Systems, inc.). In the imaging mode the fluorescence intensity was recorded by an avalanche photodiode (SPCM 200, EG&G). Fluorescence spectra were acquired by a spectrograph (SpectraPro 300i, Acton) and a liquid nitrogen cooled CCD camera (LN/CCD-100PB, 100 × 1340 pixel, Princeton) operated at 193 K.

The investigated dyes were synthesized, purified, and characterized according to ref 20.

The samples were prepared by spin coating a solution of 20 g/L polystyrene (Acros, average MW = 250000) in toluene (Merck, Uvasol) with a dye content of $\sim 10^{-11}$ M on a microscopy cover slide. To minimize the background due to luminescent impurities, we irradiated the polystyrene solution with intense white light. Further the cover slides were kept in chromosulfuric acid and rinsed with water (tridest) and Methanol (Merck, Uvasol) just before use. By negative control we confirmed that fluorescent impurities were negligible.

Dyes were checked for purity by reversed phase HPLC (Varian) with a diode array absorbance spectrometer (TIDAS, J&M) as a detector.

Aggregation of dye molecules was ruled out by standard aggregation tests in both polar (methanol) and nonpolar solvents (toluene) performed over orders of magnitude of dye concentration. Sample preparation and single-molecule experiments were carried out at room temperature in nitrogen atmosphere. The excitation power was in the order of $1 kW/cm^{-1}$ which is well below the fluorescence saturation intensity. Fluorescence intensity images were obtained by raster scanning the sample. From these images separated fluorescence spots were chosen for the investigation. The spectral sequences were recorded as a rapid succession of single molecule spectra with less than 20 ms time lag between each. A background spectrum, recorded under current conditions with respect to excitation power, integration time, etc., was subtracted from each spectrum. To determine the wavelengths of the fluorescence maxima systematically and with better accuracy, spectra were smoothed by convolution of the raw data with a normalized Gaussian distribution.

$$\bar{I}(\lambda) = \int I(\lambda')\, G(\lambda' - \lambda) \mathrm{d}\lambda' \qquad (1)$$

where $\bar{I}(\lambda)$ and $I(\lambda')$ are the smoothed and the raw spectra and $G(\lambda' - \lambda)$ is the normalized Gaussian. The bandwidth σ of the applied Gaussian distribution was 3 nm, which is sufficient to smooth the noise at the spectral band maxima but still much narrower than the minimal observed width of vibronic bands. Raw and smoothed data is exemplarily presented in Figure 1. For better perceptibility smoothed spectra are displayed in all sequences.

Results and Discussion

Sorting Single-Molecule Spectra. We have recorded spectral sequences of 9-amino-N−(2,6-diisopropylphenyl)perylene-3,4-dicarboximide (in the following: API, Figure 2a) and its derivative *N*,*N*-di(*tert*-butoxycarbonyl)-API (in the following: DAPI, Figure 2b). One hundred five API and 166 DAPI molecules were investigated, yielding a total of 6075 and 6940 single-molecule spectra, respectively. Representative single molecule fluorescence spectra are presented in Figure 2. Single molecule fluorescence spectra of API show three substantially different forms of appearance with respect to shape and spectral position, whereas DAPI shows two spectral types, each corresponding to one API form of appearance. We find (1) type I fluorescence spectra with three distinct vibrational emission bands at ~ 530, ~575, and ~620 nm with energy gaps relative to the 0→0 transition of ~1400 and ~2800 cm^{-1}; (2) broad, unstructured type II fluorescence spectra with a wide distribution of their spectral means and maxima; and (3) type III fluorescence spectra with distinct emission bands at ~ 620, ~680, and ~745 nm, separated by energy gaps of ~1400 and ~2700 cm^{-1}. All spectral types were found in investigations on API, only type I and type III in those on DAPI.

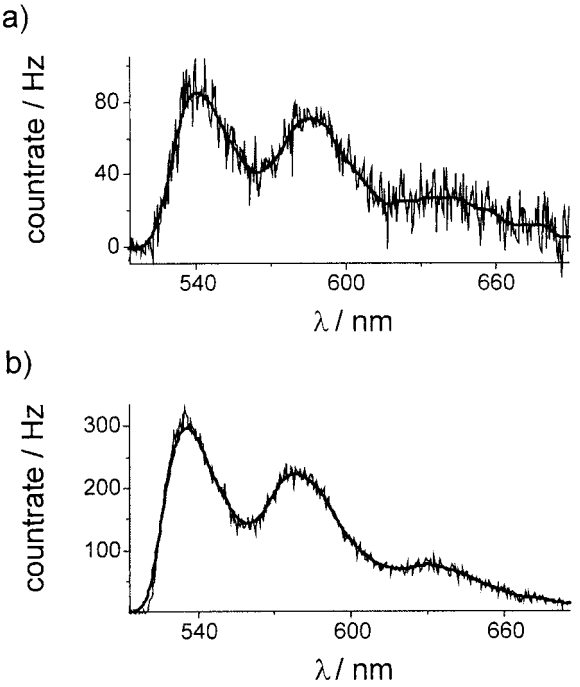

Figure 1. Two exemplarily single molecule fluorescence spectra of moderate intensity, both displayed as raw and smoothed data. Spectrum (a) was taken from the sequence shown in Figure 4, spectrum (b) is the type I spectrum in Figure 2b.

By performing the described precautions trivial artifacts, like contaminants and aggregation of dye molecules, can be virtually excluded as origin of the spectral multiplicity. In particular, a sole API chromophore can emit both type I and type II spectra, as transitions between these spectral forms of appearance evidence.[19]

The spectral type I (Figure 2), predominantly observed for both dyes, corresponds excellently with DAPIs, but not with APIs bulk fluorescence spectrum in toluene. The infrequently observed spectral type II agrees with the bulk properties of API. This spectral type is absent in the case of DAPI. Spectral type I and II can be attributed to two different conformations of the amino group relative to the chromophore. Spectral type I originates from conformers with interrupted resonance (off-resonance conformer) between chromophore and amino lone pair, type II originates from in-resonance conformers. Type II spectra are not found for DAPI in accordance with the sterically demanding substituents forcing the amino lone pair out of the chromophore's π-system. The seemingly missing correspondence between the frequency of observation of the spectral types and the bulk spectrum in studies on API is the consequence of

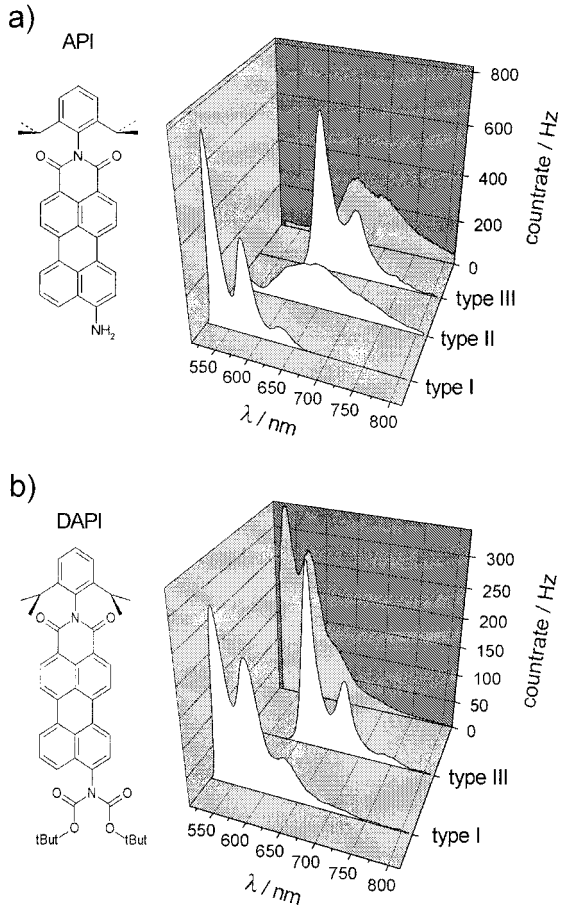

Figure 2. Structures and the observed types of single molecule fluorescence spectra of the investigated dyes, the respective ensemble spectra in toluene are displayed in arbitrary units in the back. The excitation wavelength was 514.5 nm, acquisition time per spectrum was 1 s. (a) Representative API fluorescence spectra. Type I: off-resonance spectrum with characteristic vibronic maxima at about 534, 575, and 620 nm. Type II: in-resonance spectrum with characteristic unstructured band shape, bathochromically shifted and considerably less intense relative to type I spectra. Type III: characteristic spectrum with fluorescence maxima at about 618 and 677 nm. (b) Representative fluorescence DAPI spectra. Type I: off-resonance spectrum with characteristic vibronic maxima at about 537, 578, and 628 nm. Type III: characteristic spectrum with fluorescence maxima at about 617 and 676 nm. Type II spectra were not observed.

the considerably lower fluorescence quantum yield of the in-resonance conformer, resulting in a strong underrepresentation of the in-resonance conformer in our data set. The quantum yields of fluorescence of API and DAPI were in bulk experiments determined to be 0.2 and 0.7. A detailed description of the assignment of spectral types to conformers and the cause of the missing correspondence between bulk and single molecule spectra is given in ref 19. The origin of spectral type III, found for both dyes, is yet unknown, but its vibronic progression matches the isolated 0→2 and 0→3 transitions of type I spectra.

The previous examples demonstrate how the investigation of individual molecules can reveal small populations of spectrally different forms of one dye typically hidden in the ensemble spectrum.

According to antivalent physical criteria the molecules of an ensemble can be divided into groups with distinctive molecular properties. These groups will be called subensembles. As seen for the various spectral types, the frequency of finding molecules belonging to a certain subensemble in single molecule experiments does not necessarily reflect the fraction of the respective

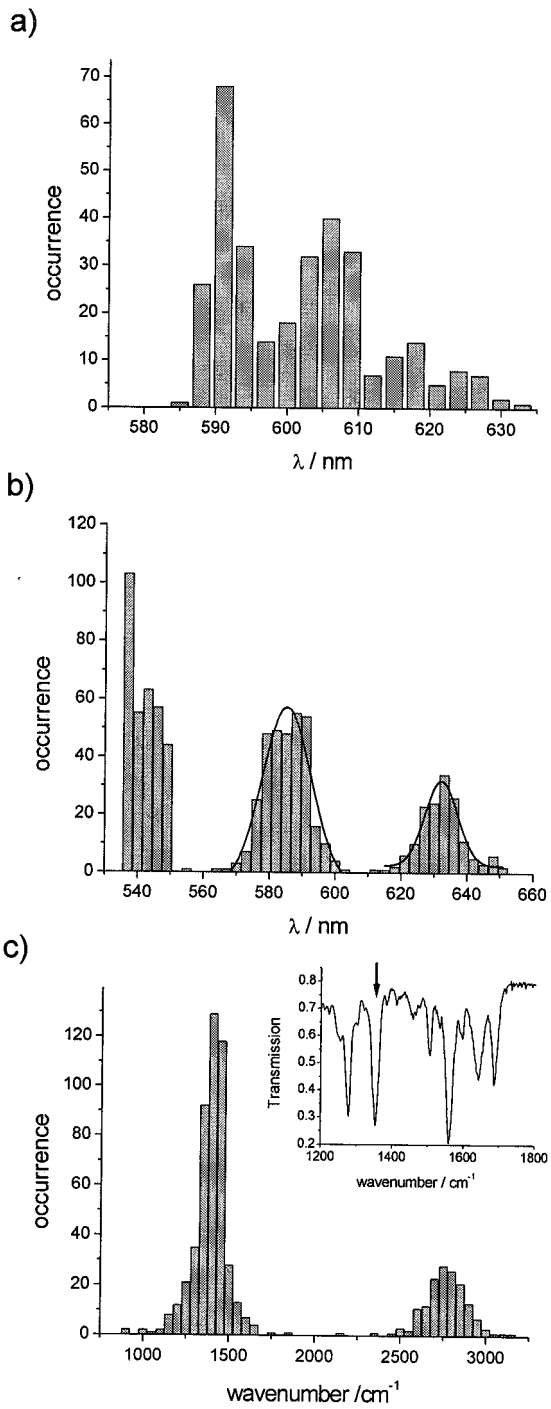

Figure 3. Histograms of different spectral features of the selected (see text) API type I spectra. Acquisition time per spectrum was 1 s. (a) Distribution of spectral means (step size 3 nm). (b) Distribution of vibronic maxima wavelength's (step size 3 nm). A Gaussian fit yields bandwidths of about 13 nm for the distribution of each vibronic band. The states found in (a) do not differ in the fluorescence maxima positions, as each vibronic band exhibits an unstructured distribution of maxima. The accumulation at 534 nm may still be an artifact caused by the influence of the dichroic mirror. (c) Distribution of energy gaps between the vibronic band maxima (step size 50 cm^{-1}). By relating the transition maxima to each other a precise insight into the vibronic structure of the API ground state was achieved. The maximum at 1380 cm^{-1} originates from the energy gap between the ground and first as well as the first and the second vibronic level, the maximum at 2760 cm^{-1} from the energy gap between the ground and second level. A vibration of 1360 cm^{-1} is also found in the IR spectrum of API (see inset).

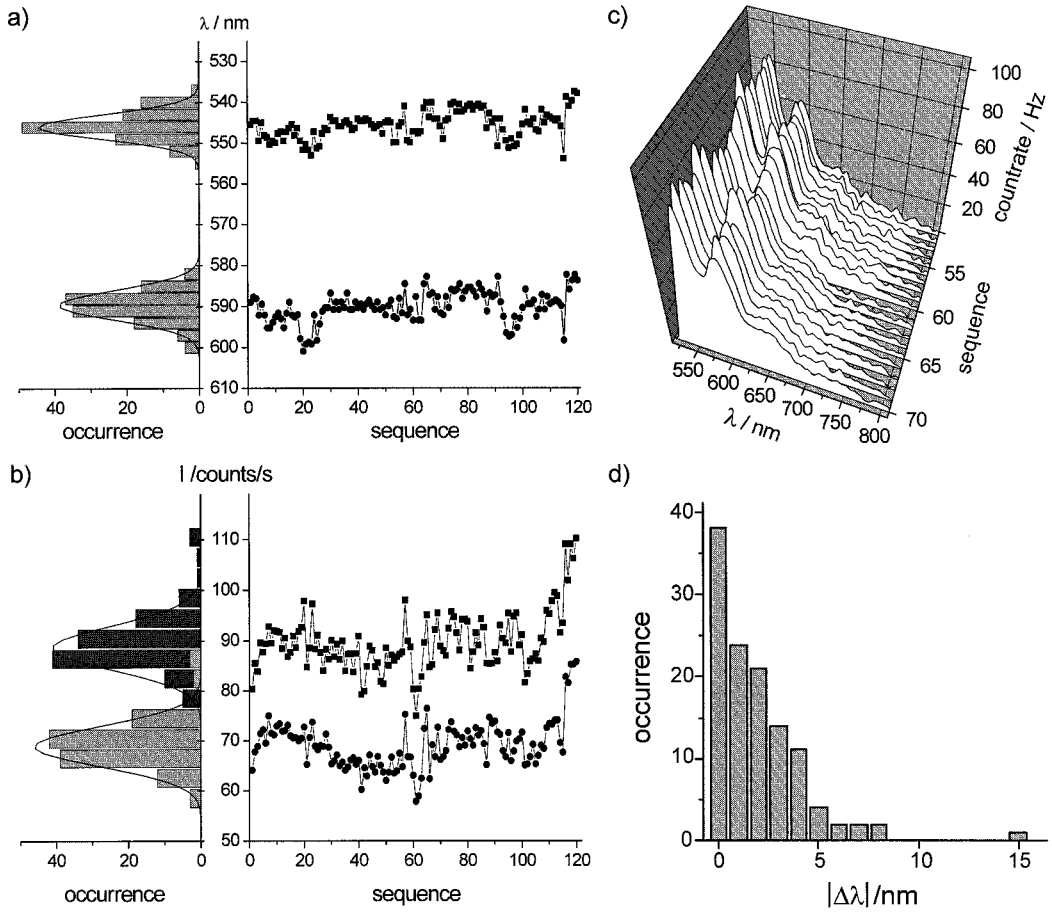

Figure 4. Spectral diffusion of the fluorescence spectra of a single API molecule. Presented are the temporal trajectories of the vibronic band maxima positions and intensities, respective histograms and a section of the spectral sequence. Acquisition time per spectrum was 1 s. (a) The histogram of spectral maxima positions of each vibronic band (gray bars, step size 3 nm) shows a statistical distribution (the solid line is a Gaussian fit), evidencing spectral diffusion. (b) The histogram of spectral maxima intensities of each vibronic band (step size 4 Hz) shows a statistical distribution (the solid line is a Gaussian fit), evidencing intensity diffusion. A correlation between the trajectories of the two vibronic bands is cognizable for both quantities. There is no correlation between the quantities. (d) Distribution of absolute spectral shift width. The temporal trajectories of the 0→0 band maximum of the spectral series shown in Figure 4a was analyzed. The absolute values of the spectral shifts from one spectrum to the next were plotted into a histogram.

molecules in the ensemble. This is particularly the case if the selection criterion, the detectability by sufficient fluorescence intensity in our case, and the division criterion, the spectral type in our case, are correlated.

Analysis of the Vibronic Progression. The spectra of the subensembles I and III have clearly resolved vibronic progressions allowing a more detailed analysis. In the following we focus especially on features common to one spectral type, and hence are specific to the respective subensemble, as opposed to statistical deviations leading to an inhomogeneous distribution. Figure 3 displays histograms obtained from one set of type I single molecule fluorescence spectra of API. Since a considerable fraction of spectra is truncated on the short wavelength edge by the dichroic mirror, only spectra with 0→0 transition band maxima at $\lambda \geq 534$ nm were selected to avoid a systematic error in the analysis. This reduces the number of type I spectra to a total of 322 obtained from 14 single API molecules.

The distribution of the spectral means (Figure 3a) shows different accumulations. The histogram of spectral positions of the vibronic maxima (Figure 3b) has three well separated accumulations corresponding to the three vibronic bands of the type I spectrum in Figure 2. The width of the accumulations centered at 585 nm and 632 nm reflects the inhomogeneous spectral distribution of positions of the spectral bands and is considerably narrower than the distribution of the spectral means (Figure 3a). Any further internal structure in these accumulations is missing, indicating that the accumulations in Figure 3a result from differences in the shapes of type I spectra.

Figure 3c shows a histogram of the energy gaps of the vibronic bands relative to each other, calculated for every single molecule spectrum and reveals two distinctive distributions. The first one at 1380 cm^{-1} results from the energy gap between the 0→0 and 0→1 transition as well as from the 0→1 and 0→2 transition, the second one at 2760 cm^{-1} from the energy gap between the 0→0 and 0→2 transition. Because both the energy gap between the 0→0 and the 0→1 transition and the 0→1 and 0→2 transition are isoenergetic and the energy gap between the 0→0 and 0→2 transition has twice the energetic distance, the respective oscillator must be harmonic in the range of the first vibronic levels of the ground state. From a comparable analysis of DAPI we obtained energetic gaps of 1450 and 2850 cm^{-1}. Furthermore, two vibronic bands separated by an energy gap of about 1400 cm^{-1} were found in type III spectra of API as well as DAPI. This agrees well with the IR spectra (see inset in Figure 3c) of both dyes, exhibiting an absorption band at 1360 cm^{-1}.

Spectral Dynamics. Both dyes show a remarkable variety of dynamic behavior in their spectral sequences.

The possibility to resolve the vibronic bands in type I and type III spectra provides the opportunity for a more detailed

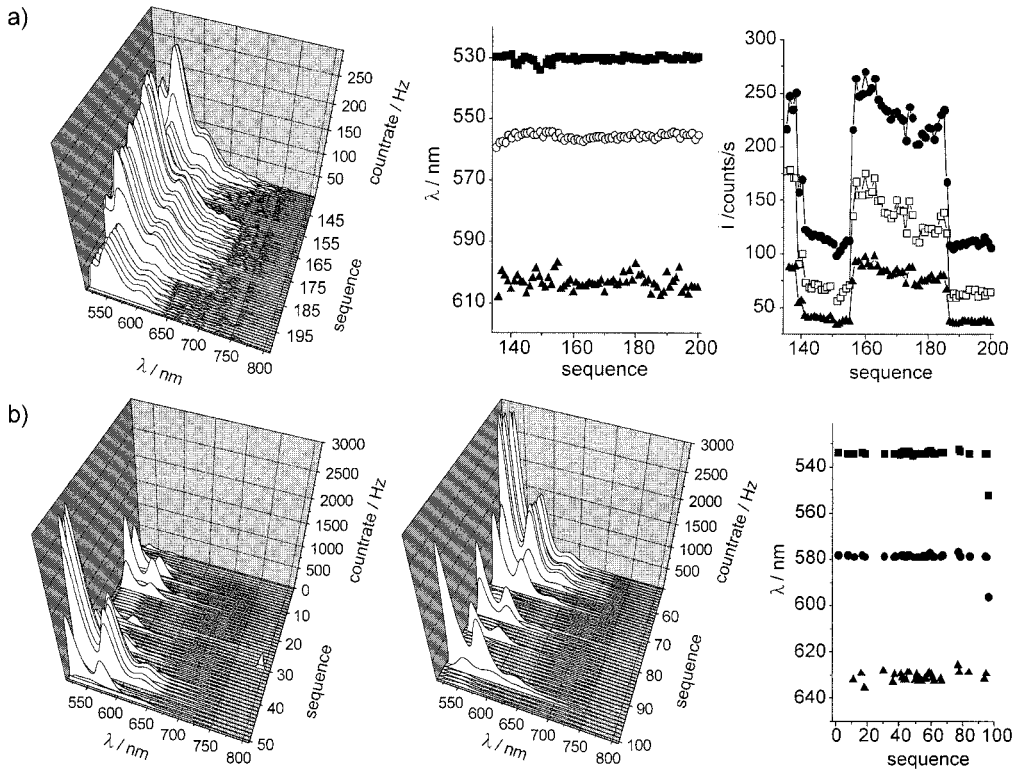

Figure 5. (a) Intensity jumps of a single DAPI molecule. Repeated intensity jumps between two states, possessing significantly different emission rates. Because no change in the fluorescence's spectral shape and position can be observed, a shift of the absorbance spectrum can be excluded as cause of the intensity change. (b) Reversible photobleaching of a single API molecule, resolved in the spectral domain. Obviously reversible photobleaching is just a particular case of intensity jumping, with one state being quasi nonfluorescent. Spectral position and band shape recur each time the molecule is in the emitting state. In both cases the acquisition time per spectrum was 1 s.

phenomenological description and classification of spectral dynamics. To sort the multitude of fluorescence fluctuations we have classified them according to two major criteria: (1) the trajectory of the analyzed quantity (spectral mean, spectral position of intensity maxima, intensity of vibronic bands, etc.), indicating whether a quantity jumps between distinct values (*transitional*) or fluctuates randomly (*diffusional*), and (2) the effect on the respective quantities, indicating if a change appears only in the intensity of the fluorescence spectra or also in their shape. We will call any kind of random fluctuation of a molecular property *diffusion*. Such processes are typically characterized by a Gaussian distribution of the observed quantity. In accordance with the common use, random fluctuations associated with the spectral shape or position will be called *spectral diffusion*. In analogy random fluctuations of the emission rate will be termed *intensity diffusion.*

An example of spectral diffusion in a sequence of type I spectra of an API molecule is shown in Figure 4. The trajectories of the spectral positions for the vibronic bands fluctuate randomly and their distribution agrees well with a Gaussian (Figure 4a). Significant random fluctuations of the intensity at the band maxima of the spectra are also visible in the displayed section (Figure 4b). Intensity diffusion occurs independently from spectral diffusion in this case as no correlation between the intensity and the spectral positions was found. Spectral and intensity diffusion may originate from environmental processes such as microenvironment dynamics,[21−24] interactions with impurities diffusing through the matrix,[25] as well as spatial and orientational migration of the dye molecule.[26−29]

Contrary to random fluctuations are transitional processes, for which the distribution of the respective observable exhibits two or more accumulations. We will call any kind of transitional processes in single-molecule spectroscopy *jumps*. In analogy to the above definition, transitions affecting solely the fluorescence intensity will be called *intensity jump*. Any other transition will be denoted as *spectral jump.* In Figure 5 we present pure intensity jumps resolved in the spectral domain. Figure 5a shows a single DAPI molecule switching between two states of different fluorescence intensity, while the band shape and the spectral position of the intensity maxima is unchanged in both states. Jumps into a nonemitting state are a special case of intensity jumps and are well-known from intensity trajectory measurements.[11,30−35] This behavior is usually called "*blinking*" or "*reversible photobleaching*", depending on the off states' duration. Figure 5b shows repeated "blinking" of a single API molecule. A transition of the molecule into the triplet state as explanation for dark intervals is unlikely here due to the long duration of these non emitting intervals. The spectral position and band shape recurs each time the molecule is in the emitting state. During the dark intervals the fluorescence must be reduced by enhanced radiationless desactivation not by a reduced absorption cross section due to a spectral shift.[36] A shift of the absorbance spectrum should result in a simultaneous shift in the fluorescence spectrum, yet this is not visible. Furthermore, at room temperature, contrary to cryogenic temperature, fluorescence spectra are significantly broadened, so that a shift out of excitation resonance is unlikely. It is further unlikely that the observed behavior originates from repeated orientational jumps into a position where the transition dipole moment is perfectly parallel to the incident excitation light beam.

In Figure 6b an example for a spectral jump as large as 27 nm is presented. Clearly visible is a bathochromic shift of the fluorescence spectra accompanied by a considerable drop in the emission rate and in resolution of the vibronic progression. The trajectory of the spectral position of the vibronic intensity maxima is plotted and the respective distributions show two

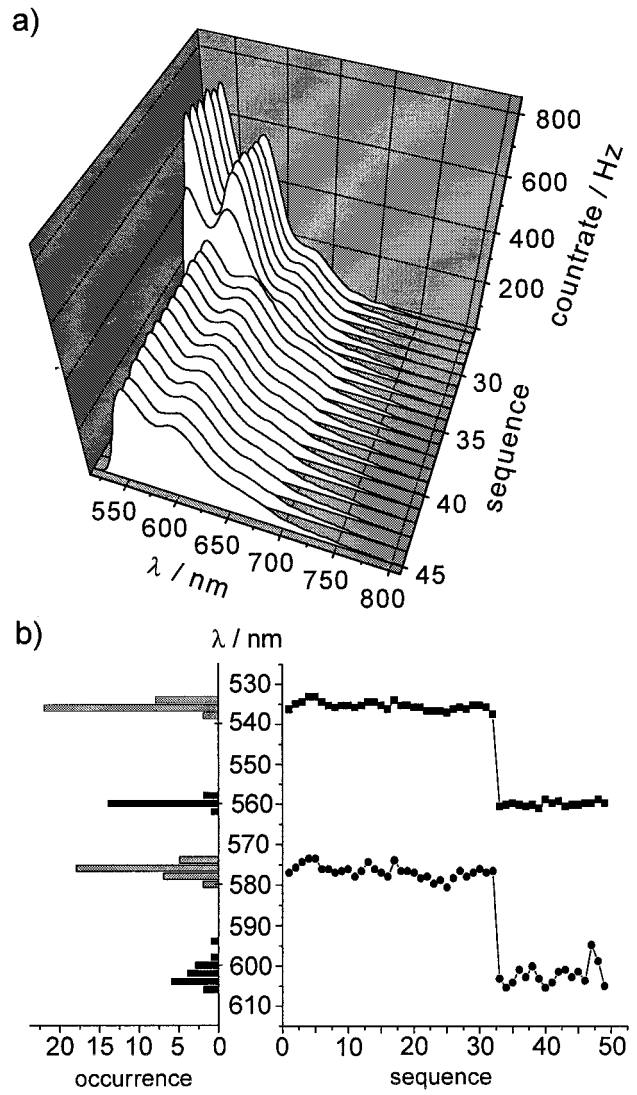

Figure 6. Bathochromic spectral jump (example where spectral shifting, S1-mechanism, is visible) of the fluorescence spectra of a single DAPI molecule. Presented are the temporal trajectories of the vibronic band maxima positions, respective histograms and a section of the spectral sequence. Acquisition time per spectrum was 1 s. The spectral shift occurs abruptly in spectrum no. 8, resulting separated accumulations in the histogram of the maxima wavelength's distribution before and after the jump. This evidences the transition between two molecular or supramolecular states. The fluorescence spectrum is 760 cm^{-1} bathrochromically shifted, while the energy gap between the band maxima remains constant at 1260 cm^{-1}. The spectral shift is accompanied by a significant decline in intensity.

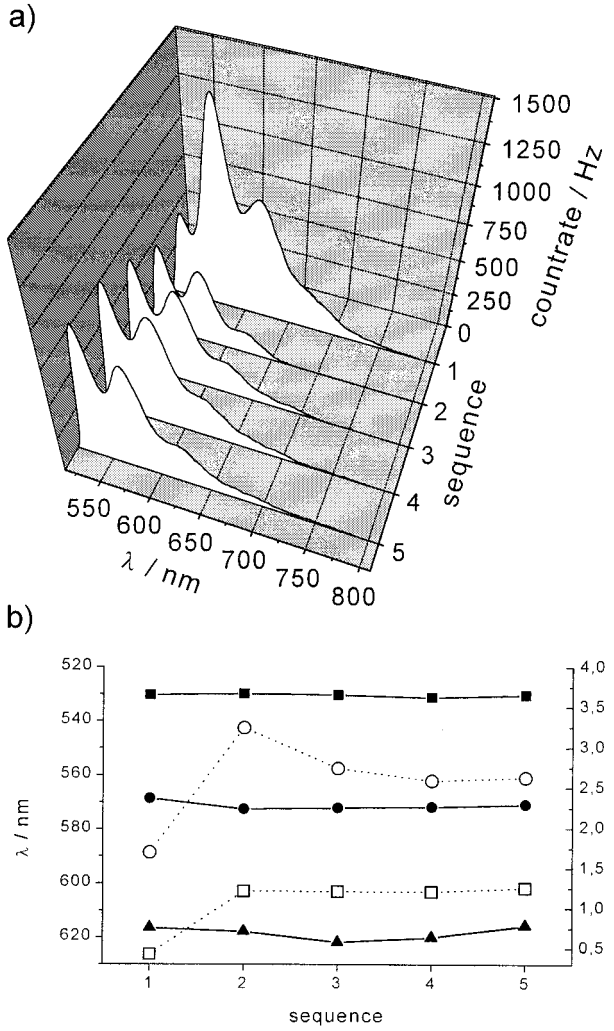

Figure 7. (a) Example where spectral seesawing (S2-mechanism) is visible. A drastic change in the ratio of the vibronic band intensities occurs from spectrum 1 to spectrum 2. (b) A chart of the distinct band maxima wavelengths (solid symbols) and the intensity ratios (open symbols) vs the acquisition sequence. The band maxima positions remain constant, whereas the intensity ratios change significantly after spectrum 1. Acquisition time per spectrum was 1 s. A model to explain this behavior by a variation of the Franck−Condon Factors is given in Figure 8b.

strictly separate accumulations for each vibronic band. The width of these accumulations reflects the extent of the superimposed spectral diffusion.

Another example of a spectral jump, but of substantially different nature, is presented in Figure 7. The spectral positions of the vibronic band maxima remain constant, whereas their intensity ratios change significantly. This can be described by a variation of the Franck−Condon factors leading to a shift of the spectral mean although the spectral positions of the vibronic bands stay rather constant.

Any diffusional and transitional spectral dynamic in the spectral subensembles can be interpreted as a superposition of intensity variations (I-processes) and four idealized basic spectral phenomena (S-processes):

1. Spectral *shifting* (S1) without changes in the spectral shape (Figure 8a). This behavior originates from a variation in the energetic distance between the S_0- and S_1-potential wells, while the hypersurfaces' shapes remain unchanged. Spectral shifts have frequently been observed.[37−40]

2. Spectral *seesawing* (S2), this term describes variations of the intensity ratios within the vibronic progression (Figure 8b). The underlying variations of Franck−Condon Factors is caused by an isoenergetic displacement of the S_0- and S_1-potential wells relative to each other.

3. Spectral *stretching* (S3) of the fluorescence spectrum results from a change in the energetic separation of the vibronic progression (Figure 8c), originating from a change in width and slope of the groundstate potential well.

4. A change in the resolution of the vibronic progression (S4).

We found a large number of spectral sequences where the introduced mechanisms could be distinguished. A variety of combinations of S-mechanisms was observed in individual jumps. Almost any spectral change was found to be accompanied by an intensity jump, yet intensity jumps are not necessarily associated with a spectral jump (see Figure 5). In Figure 6 spectral shifting is visible, accompanied by a significant

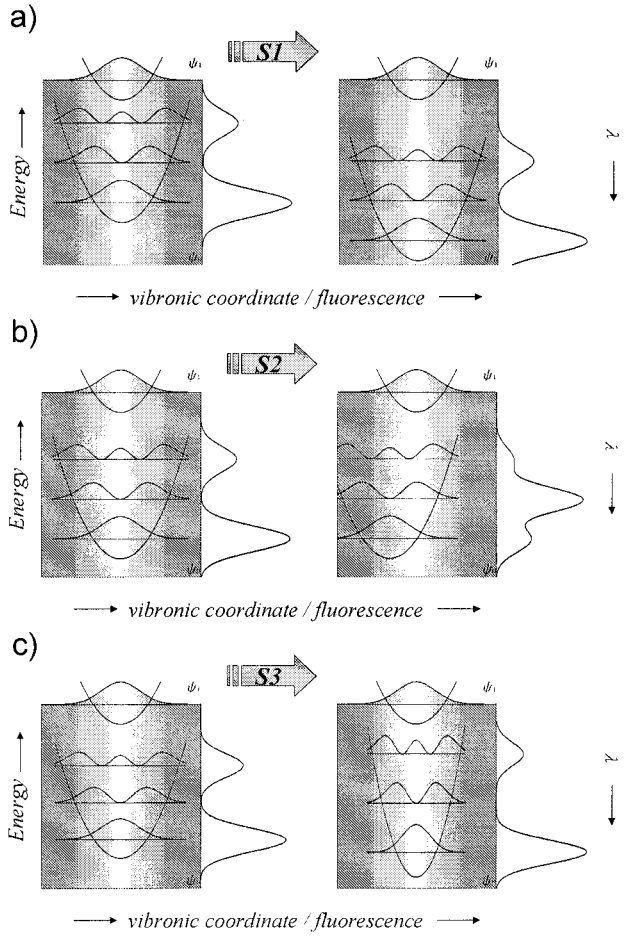

Figure 8. Idealized schemes illustrating the relation between molecular processes and spectral events. The assumption of a harmonic oscillator is in good agreement with our results regarding type I spectra. (a) Shifting of single molecule spectra (S1-mechanism). An isostructural variation in the energetic distance between ground and excited state leads to a pure spectral shift without variations in the fluorescence band shape. An example for spectral shifting is given in Figure 4. (b) Seesawing of single molecule API spectra (S2-mechanism). An isoenergetic displacement of the ground and excited-state potential well relative to each other leads to a variation in the Franck−Condon Factors. This is observed as a change in fluorescence band intensity ratios. An example for seesawing is given in Figure 7. (c) Stretching of single molecule spectra (S3-mechanism). A deformation of the ground-state potential well leads to a variation in the energetic distances of the vibronic progression. This causes a change in the spectral distance of the vibronic fluorescence bands.

change in the resolution of the vibronic progression and in the intensity (S1, S4, I), whereas the shape of the spectra stays almost unchanged in the sequence displayed in Figure 5 while the intensity jumps considerably (I). An example with obvious spectral seesawing in combination with an intensity drop (S2, I) is shown in Figure 7. No clear example for spectral stretching (S3) was found yet.

Single molecule spectral dynamics can formally be divided into processes originating from changes within the chromophore and changes of the chromophoric environment, hence are intrinsically and extrinsically induced. For example intersystem crossing and conformational jumps are typical intrinsic, whereas externally applied fields, such as in the Stark effect, and changes of the microenvironment are extrinsic processes. Intrinsic conformational transitions between spectral type I and II of API were described in ref 19. In a crystalline as well as in an amorphous host like a polymer, diffusion and spectral events which are only observed for one individual molecule (individual spectral events) can most likely be attributed to extrinsic origins. On the other hand, in an amorphous host specific events observed uniformly for different molecules despite their individual environments, indicate an intrinsic mechanism. Contrary in a crystalline host recurring events may have intrinsic as well as extrinsic origin, due to the identical molecular proximity.[41]

Conclusion and Outlook

Even rather small fluorescent dyes, such as API and DAPI embedded in an amorphous solid, exhibit a large variety in spectral appearance and dynamics. The underlying molecular processes are rarely known and are likely to vary from one dye−host system to another. As single molecule fluorescence experiments are nowadays established in many scientific fields, such as molecular biology and material science, a deeper insight into the molecular and intermolecular effects, influencing a fluorophore's spectrum, is of elementary relevance. In this work spectral phenomena and dynamics were systematically characterized, classified, and statistically surveyed to approach their origins in the case of the investigated aminoperylen/polystyrene system. The analysis of the peculiarities of spectral fluctuations lead to implications about displacements and distortions in the potential wells of the respective molecule's hypersurfaces. A statistical survey helps to localize the origin of an observed dynamic within or outside the chromophore. By investigating larger data sets, deliberate modification of the dye−host system, adapted bulk experiments and by comparison to calculated scenarios a deepened insight into molecular and intermolecular processes, affecting the fluorescence behavior of a dye molecule, will be accessible.

References and Notes

(1) Xie, X. S.; Trautman, J. K. *Annu. Rev. Phys. Chem*. **1998**, *49*, 441.
(2) Weiss, S. *Science* **1999**, *283*, 1676.
(3) Moerner, W. E.; Dickson, R. M.; Norris, D. J. *Adv. At. Mol. Opt. Phys.* **1998**, *38*, 193.
(4) Ambrose, W. P.; Goodwin, P. M.; Jett, J. H.; Van Orden, A.; Werner, J. H.; Keller, R. A. *Chem. Rev.* **1999**, *99*, 2929.
(5) Lu, H. P.; Xie, X. S. *Int. J. Res. Phys. Chem. Chem. Phys.* **1999**, *2*, 59.
(6) Brasselet, S.; Moerner, W. E. *Single Mol.* **2000**, *1*, 17.
(7) Schenter, G. K.; Lu, H. P.; Xie, X. S. *J. Phys. Chem. A* **1999**, *103*, 10477.
(8) Deniz, A. A.; Laurence, T. A.; Beligere, G. S.; Dahan, M.; Martin, A. B.; Chemla, D. S.; Dawson, P. E.; Schultz, P. G.; Weiss, S. *Proc. Natl. Acad. Sci. U.S.A.* **2000**, *97*, 5179.
(9) Ha, T.; Zhuang, X. W.; Kim, H. D.; Orr, J. W.; Williamson, J. R.; Chu, S. *Proc. Natl. Acad. Sci. U.S.A.* **1999**, *96*, 9077.
(10) Hofkens, J.; Maus, M.; Gensch, Th.; Vosch, T.; Cotlet, M.; Kohn, F.; Herrmann, A.; Müllen, K.; De Schryver, F. C. *J. Am. Chem. Soc*. **2000**, *122*, 9278.
(11) Dickson, R. M.; Cubitt, A. B.; Tsien, R. Y.; Moerner, W. E. *Nature* **1997**, *388*, 355.
(12) Widengren, J.; Mets, U.; Rigler, R. *J. Phys. Chem*. **1995**, *99*, 13368.
(13) Yip, W. T.; Hu, D.; Yu, J.; Vanden Bout, D. A.; Barbara, P. F. *J. Phys. Chem. A* **1998**, *102*, 7564.
(14) Weston, K. D.; Carson, P. J.; De Aro, J. A.; Burrato, S. K. *Chem. Phys. Lett* **1999,** *308*, 58.
(15) Edman, L.; Foldes-Papp, Z.; Wennmalm, S.; Rigler, R. *Chem. Phys*. **1999**, *247*, 11.
(16) Ha, T.; Laurence, T. A.; Chemla, D. S.; Weiss, S. *J. Phys. Chem. B* **1999**, *103*, 6839.
(17) Bopp, M. A.; Sytnik, A.; Howard, T. D.; Cogdell, R. J.; Hochstrasser, R. M. *Proc. Natl. Acad. Sci. U.S.A.* **1999**, *96*, 11271.
(18) Kohn, F.; Hofkens, J.; De Schryver, F. C. *Chem. Phys. Lett*. **2000**, *321*, 372.
(19) Stracke, F.; Blum, C.; Becker, S.; Mullen, K.; Meixner, A. J. *Chem. Phys. Lett*. **2000**, *325*, 196.
(20) Becker, S.; Bohm, A.; Mullen, K. *Chem. Eur. J.* **2000**, *6*, 3984.

(21) Mei, E.; Bardo, A. M.; Collinson, M. M.; Higgins, D. A. *J. Phys. Chem. B* **2000**, *104*, 9973.
(22) Talley, C. E.; Dunn, R. C. *J. Phys. Chem. B* **1999**, *103*, 10214.
(23) Yip, W. T.; Hu, D. H.; Yu, J.; Vanden Bout, D. A.; Barbara, P. F. *J. Phys. Chem. A* **1998**, *102*, 7564.
(24) Hollars, C. W.; Dunn, R. C. *J. Chem. Phys.* **2000**, *112*, 7822.
(25) English, D. S.; Furube, A.; Barbara, P. F. *Chem. Phys. Lett.* **2000**, *324*, 15.
(26) Ha, T.; Glass, J.; Enderle, T.; Chemla, D. S.; Weiss, S. *Phys. Rev. Lett.* **1998**, *80*, 2093.
(27) Ruiter, A. G. T.; Veerman, J. A.; Garcia Parajo, M. F.; Van Hulst, N. F. *J. Phys. Chem. A* **1997**, *101*, 7318.
(28) Schmidt, T.; Schutz, G. J.; Baumgartner, W.; Gruber, H. J.; Schindler, H. *Proc. Natl. Acad. Sci. U.S.A.* **1996**, *93*, 2926.
(29) Bopp, M. A.; Meixner, A. J.; Tarrach, G.; Zschokke Granacher, I.; Novotny, L. *Chem. Phys. Lett.* **1996**, *263*, 721.
(30) Jung, G.; Mais, S.; Zumbusch, A.; Brauchle, C. *J. Phys. Chem. A* **2000**, *104*, 873.
(31) Peterman, E. J. G.; Basselet, S.; Moerner, W. E. *J. Phys. Chem. A* **1999**, *103*, 10553.
(32) Haupts, U.; Maiti, S.; Schwille, P.; Webb, W. W. *Proc. Natl. Acad. Sci. U.S.A.* **1998**, *95*, 13573.
(33) Weston, K. D.; Buratto, S. K. *J. Phys. Chem. A* **1998**, *102*, 3635.
(34) Gohde, W.; Fischer, U. C.; Fuchs, H.; Tittel, J.; Basche, T.; Brauchle, C.; Herrmann, A.; Mullen, K. *J. Phys. Chem. A* **1998**, *102*, 9109.
(35) Hofkens, J.; Maus, M.; Gensch, T.; Vosch, T.; Cotlet, M.; Kohn, F.; Herrmann, A.; Mullen, K.; De Schryver, F. C. *J. Am. Chem. Soc.* **2000**, *122*, 9278.
(36) Fleury, L.; Sick, B.; Zumofen, G.; Hecht, B.; Wild, U. P. *Mol. Phys.* **1998**, *95*, 1333.
(37) Pirotta, M.; Renn, A.; Werts, M. H.; Wild, U. P. *Chem. Phys. Lett.* **1996**, *250*, 576.
(38) Lu, H. P.; Xie, X. S. *Nature* **1997**, *385*, 143.
(39) Wang, H.; Bardo, A. M.; Collinson, M. M.; Higgins, D. A. *J. Phys. Chem. B* **1998**, *102*, 7231.
(40) Weston, K. D.; Carson, P. J.; Metiu, H.; Buratto, S. K. *J. Chem. Phys.* **1998**, *109*, 7474.
(41) Kulzer, F.; Kummer, S.; Matzke, R.; Brauchle, C.; Basche, T. *Nature* **1997**, *387*, 688.